Measuring absolute spectral radiance using an erbium-doped fiber amplifier

Bruno Sanguinetti,[*] Thiago Guerreiro, Fernando Monteiro, Nicolas Gisin, and Hugo Zbinden

Group of Applied Physics, University of Geneva, Chemin de Pinchat 22, CH-1211 Geneva 4, Switzerland

We describe a method to measure the spectral radiance of a source in an absolute way without the need of a reference. Here we give the necessary detail to allow for the device to be reproduced from standard fiber-optic components. The device is suited for fiber-optic applications at telecom wavelengths and calibration of power meters and spectrometers at light levels from 1 nW to 1 μW.

I. INTRODUCTION

Measurement of optical power, although extremely common in both industry and research, remains relatively inaccurate with standard commercial equipment having nominal uncertainties of the order of 5%. In a metrology laboratory, an absolute standard such as a cryogenic radiometer can achieve accuracies of 10^{-4} for visible collimated laser radiation [1]. Fiber-coupled systems have also been demonstrated [2–4]. This type of experiment however requires considerable time and effort and is usually not available at the site where the measurement is needed. The accuracy of the calibration chain then limits the overall accuracy of the measurement to values which are typically of the order of 1%. Comparisons of power meters from different metrology laboratories yield discrepancies of the order of 10^{-3} [1,5].

Furthermore, these accuracies are obtained for relatively high incident powers, of the order of 10^{-3} W. This is more than 10 orders of magnitude away from powers used in applications at the quantum level, where the energy of a photon is typically of the order of 10^{-19} J. Recent advancements in the field of quantum optics and single-photon detectors has motivated work on accurate measurements at low powers [6,7], and their comparison with classical cryogenic radiometers [8,9].

We have recently demonstrated that the fidelity of a cloning process in an erbium-doped fiber amplifier is related to the amount of input light into the fiber [10]. This approach is conveniently based on fundamental laws of nature. However, it requires a polarimetric measurement which limits the precision of the results.

Here we present an alternative method for absolutely measuring the radiance of a source. This method consists in comparing the spontaneous emission of an erbium amplifier to the emission stimulated by the source. Using spontaneous emission as a standard was originally proposed in [11,12], and has been implemented using spontaneous parametric down-conversion (SPDC) in bulk crystals [13,14], but the free-space nature of the setup makes it challenging to accurately count the number of spatial modes involved. Furthermore the radiances and gain that can be achieved in bulk crystals remain low.

This article in divided into four sections. In Sec. II we explain the working principle of the radiometer. Section III describes the experimental setup including the details and characterization of the individual components. Section IV

---

*bruno.sanguinetti@unige.ch

details the steps taken during a single measurement run. Finally we estimate errors and discuss our results in Sec. V.

II. WORKING PRINCIPLE

Spontaneous emission in an inverted atomic medium can be seen as being stimulated by vacuum fluctuations. These fluctuations can serve as an "omnipresent standard," as shown in [13,15]. Indeed, the spontaneous emission corresponds to the emission stimulated by exactly one photon per mode.

A specific atomic medium such as an erbium-doped fiber will have a gain G defined by [10]

$$G = \frac{\partial \mu_{\text{out}}}{\partial \mu_{\text{in}}}, \tag{1}$$

where μ_{in} and μ_{out} are the number of input and output photons per mode. The smallest value of gain is $G = 1$, representing a medium for which the output equals the input. Using this definition, and assuming no loss, the number of output photons per mode μ_{out} is

$$\mu_{\text{out}} = G\,\mu_{\text{in}} + G - 1, \tag{2}$$

where the term $G\,\mu_{\text{in}}$ represent the emission stimulated by the input light, and the term $G - 1$ represents the spontaneous emission μ_0. These unitless values can be converted into an optical power by multiplying them by the photon energy $h\nu$ and by the number of modes per second N, which is the inverse of the coherence time of the light: $N = 1/\tau_c$ [16].

When measuring the spontaneous and stimulated emissions with an uncalibrated but linear power meter, the reading will be off by a constant k with respect to the real value. The measured values P_{sp}^* and P_{st}^* are respectively

$$P_{\text{sp}}^* = (G - 1)\frac{h\nu}{\tau_c}k, \tag{3}$$

$$P_{\text{st}}^* = (G\,\mu_{\text{in}} + G - 1)\frac{h\nu}{\tau_c}k. \tag{4}$$

Equations (3) and (4) can be solved to obtain μ_{in} independently from the power meter calibration factor k:

$$\mu_{\text{in}} = (1 - 1/G)(P_{\text{st}}^*/P_{\text{sp}}^* - 1). \tag{5}$$

We stress that the only assumption used to arrive at Eq. (5) is that the power meter is linear. According to Eq. (1) the gain G can also be measured exactly with the same uncalibrated linear power meter rendering the measurement of μ_{in} absolute. The
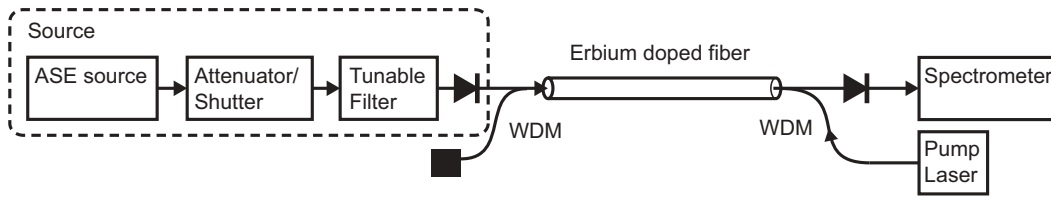

FIG. 1. Experimental setup. A stable ASE source is filtered and injected into a fully inverted erbium-doped fiber. At the output of this fiber the spectrum is measured with a spectrometer. The power of the source is controlled by a variable attenuator which also contains a shutter. The diode symbols represent optical isolators which both stop back-reflections and remove any remaining 980 nm light.

power P_{in} can be evaluated from the measurement of μ_{in} as

$$P_{\text{in}} = \mu_{\text{in}} \, h \, \nu \, N \qquad (6a)$$
$$= \mu_{\text{in}} \, h \, \nu / \tau_c \qquad (6b)$$
$$= \mu_{\text{in}} \, h \, c^2 / \lambda \, l_c. \qquad (6c)$$

Unlike μ_{in}, which is unitless, P_{in} depends on the coherence time and wavelength of the photons. An absolute measurement of P_{in} then requires a standard of time or length, which can be provided with extreme accuracy by a wave meter.

We would like to note that although the experimental setup and equipment used in this experiment are different from those of the "cloning radiometer" presented in [10] the underlying principles are very similar. In [10] the spontaneous and stimulated emissions were distinguished by their polarization, whereas here they are measured at two different times.

III. EXPERIMENTAL SETUP

In this section we first give an overview of the experimental setup, and then describe each element individually. In particular we give details of the devices used, their characterization, and their contribution to the system's uncertainty.

A. Overview

The setup is shown schematically in Fig. 1. An unpolarized and stable source, based on amplified spontaneous emission, is filtered to define a specific wavelength and bandwidth. The light produced by this source is then amplified into a fully inverted single-mode erbium-doped fiber (EDF). An uncalibrated linear power meter is used to measure the gain of the fiber and a spectrometer to measure the relative spectral radiances of the spontaneous and stimulated emission.
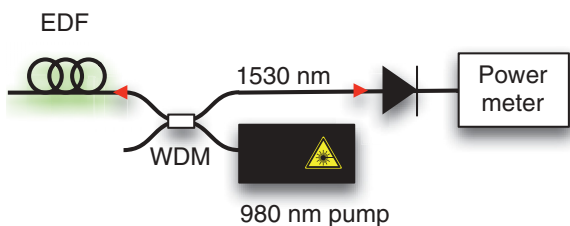

FIG. 2. (Color online) Fiber source of spontaneous emission. An erbium-doped fiber is backwards pumped. The amplified spontaneous emission counterpropagating to the pump is separated with a wavelength division multiplexer (WDM). Any residual pump light is removed using an isolator which has very strong attenuation for the pump light.

This measurement scheme is particularly robust as all losses after amplification including polarization-dependent loss are equal for both the spontaneous and stimulated emission. It is then only necessary to accurately measure the input losses of the device to obtain the spectral radiance of the source in number of photons per mode. All the fibers used support a single spatial mode and two polarization modes. Below we describe each individual element of the radiometer.

B. Source

Although this radiometer can operate with a variety of sources, we have found it useful to develop a reference source which meets the requirements of both the radiometer and subsequent calibration of a power meter. The most important aspect of the source is stability, as only with a stable source and a stable power meter it is possible to evaluate the stability of all the other elements in the setup. The source should be unpolarized in order to reduce the effect of small polarization-dependent losses. Another attractive characteristic for a source is to have a low coherence time, so that no interference due to small reflections can occur.

A spontaneous emission source based on a short erbium-doped fiber satisfies these requirements. Our setup is shown in Fig. 2. A 700 mW pump laser at 980 nm is injected into a wavelength division multiplexer (WDM) and into the erbium-doped fiber. The EDF end is angle polished to minimize back-reflections of the pump laser. The EDF is kept short in order to
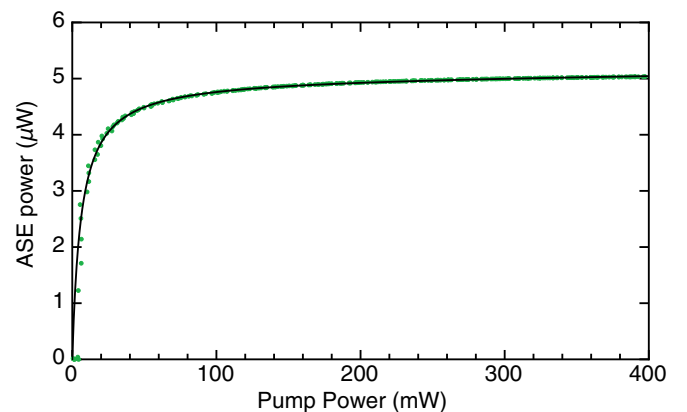

FIG. 3. (Color online) Saturation of the atomic medium. As the pump laser power P_{p} is increased the spontaneous emission power P_{ASE} increases as $P_{\text{ASE}} \propto P_{\text{p}}/(P_{\text{p}} + C)$ (fitted curve). The slope $\partial P_{\text{ASE}}/\partial P_{\text{p}}$ becomes 2000 times smaller as the pump laser power reaches 400 mW.
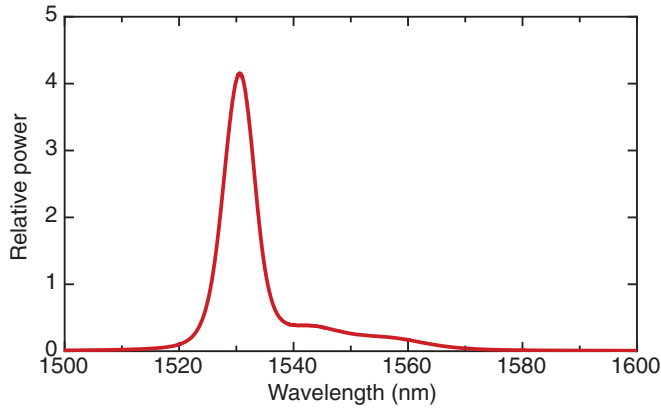
FIG. 4. (Color online) Amplified spontaneous emission spectrum. A peak is present at 1530 nm and a flat region between 1540 nm and 1544 nm.
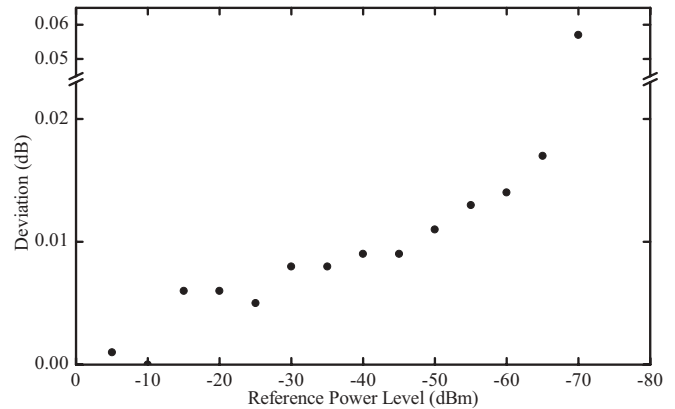

FIG. 5. Linearity of the power meter measured by METAS, the Swiss federal office of metrology. The linearity has a deviation of only 0.4% between 0 dBm and −65 dBm. The last point, at −70.1 dBm, has a deviation of 1.3% mainly due to the background noise of the power meter.

generate a sufficiently small amount of light, usable with our radiometer. Having a short EDF (1 mm to 5 cm THORLABS ER30-4/125) also ensures that only a small fraction of the pump is absorbed and that the medium is well saturated over its entire length (Fig. 3). With such a short fiber, stimulated emission is minimized and the generated light has a degree of polarization <0.5%.

Spontaneous emission at 1530 nm passes through the WDM and an isolator which plays the role of a long-pass filter removing residual pump light (Fig. 4). This source is very stable as the number of photons produced per second depends on the number of erbium ions in the fiber and their lifetime, both being constant. Although in practice the medium is only *mostly* inverted, the amplified spontaneous emission (ASE) source is over three orders of magnitude more stable than the pump laser. The source is filtered using a tunable filter (DiCon TF500) with a 1.2 nm bandwidth, and attenuated using a variable attenuator (EXFO FVA-3150) which includes an optical shutter.

C. Erbium-doped fiber amplifier

The erbium-doped fiber amplifier employed in the radiometer is of very simple construction, consisting of a short section of single-mode erbium-doped fiber in which the input light and a 980 nm pump are injected via a WDM. At the output most of the pump light is eliminated using another WDM and an isolator. For our application it is important that the medium remains fully inverted during measurement, especially at the beginning of the amplifier where loss directly influences the measurement accuracy. We chose a gain of approximately 10. On one hand, this value is low enough to guarantee that the fiber remains fully inverted, even at relatively high input powers. On the other hand, the precision required on the gain measurement is relaxed for higher gains [see Eq. (5)]. In principle it is best to pump in the forward direction to better saturate the fiber at its input; however, here we pump in the backward direction for reasons explained in Sec. IV A.

D. Power meter

The radiometer does not require a calibrated power meter; however it must be stable in time and linear. We used a Thorlabs PM100A with S154C InGaAs fiber head. The stability of the measurement was excellent: When measuring the ASE source, the Allan deviation had a minimum of 10^{-5} for time scales of one minute and stayed below 10^{-4} for days. The linearity was measured by the Swiss federal office of metrology METAS to have an error smaller than 0.4% over 60 dBm, as shown in Fig. 5.

The nominal systematic error of this power meter is 5%; this relatively high value appears to be given by the presence of reflections and interference between the fiber and the diode. Custom detectors such as traps [17–21] would perform much better in this respect.

E. Spectrometer

To acquire the spectra we used an Anritsu MS9710C spectrometer which we calibrated against a Bristol Instruments 621 wave meter. The calibration curve is shown in Fig. 6. The
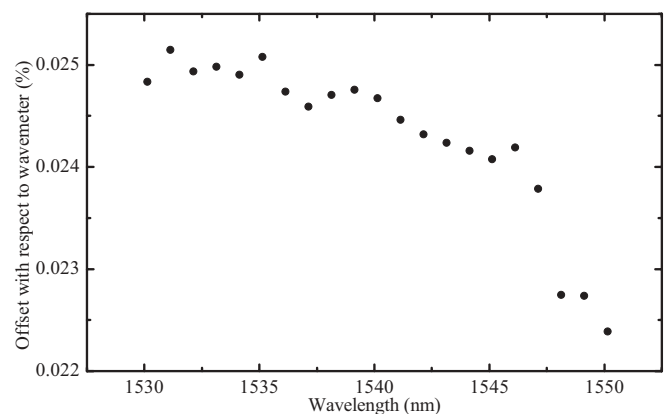

FIG. 6. Spectrometer calibration curve vs a wave meter. The calibration error is of the order of 10^{-4}. Once calibrated (linear fit) the standard deviation of the residuals is 2 pm.
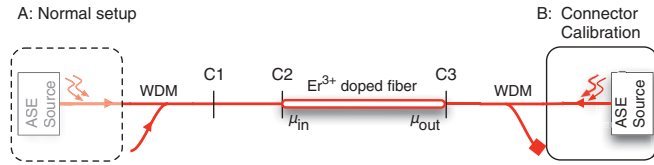
FIG. 7. (Color online) In order to calibrate the input loss of the EDF at connector C2 one injects light backwards through connector C3 and measures the amount of light P_2 out of the EDF at C2. After this, one makes the connection at C2 and measures the amount of light P_1 coming out of C1. The input loss is then P_1/P_2. This characterization is made only once since C2 will remain connected during the entire experiment.

relative wavelength error due to an uncalibrated spectrometer is of the order of 10^{-4} and will become relevant only once the power meter is improved. Once calibrated the error is of the order of 2 ppm. The linearity of the spectrometer's vertical scale was measured with respect to the calibrated power meter and found to be linear to better than 0.01 dBm, over a 30 dBm range.

F. Fibers and connectors

We used standard fibers of two different core diameters at different points of the experiment. Where only the telecom (1542 nm) light passes, SMF28 fiber was used, whereas in elements which have both telecom and 980 nm light we employed fiber components which guarantee that both wavelengths propagate in a single mode. This results in insertion loss at the interfaces between the two types of fibers.[1] However the internal loss of the telecom light in the fibers was negligible over the short lengths used in the experiment.

In order to achieve the best accuracy one should splice all the fibers, as the connections, especially APC, have loss which might change with time due to mechanical and thermal effects. In our case most fibers were connectorized in the interest of flexibility, and to better understand the limitations and stabilities of the individual elements of the experiment.

The spectral radiance $\mu_{\rm in}$ measured by the radiometer corresponds to the amount of light present at the beginning of the EDF. For this reason it is important to characterize the loss at connectors C1 and C2.

When a radiometric measurement is made, the source is in position A shown in Fig. 7. The reference light with which a power meter is calibrated is taken from C1. It is therefore important to estimate the loss at this connection. This is done with the source in position A and measuring the amount of light at C1 and then at C2. We closed the connection C1 multiple times to evaluate its repeatability and found a standard deviation between consecutive connections of 0.4%. It is possible to improve on this by only accepting the highest values for transmission as shown in Fig. 8. Using this method we reduce the error to 0.16%.

To calibrate the loss in C2 we inject reference light back through the erbium-doped fiber by putting our source in

---

[1]For interfaces between single-mode fibers, the overlap between the modes is constant; i.e., losses are stable.
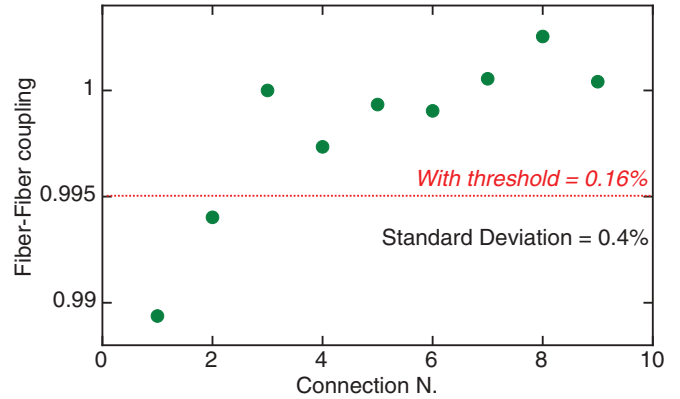

FIG. 8. (Color online) Connection statistics. Making a connection without measuring its loss each time will result in a random error. We measured this random error to be 0.4%. However it can be reduced by only accepting connections with the highest values of transmission. Rejecting values below a certain threshold we improve the repeatability to 0.16%.

position B of Fig. 7. The loss at C2 is measured after the characterization of connector C1 and introduces no random error as this connection is made only once.

IV. MEASUREMENTS

In this section we describe in detail the measurements done during a particular run of the experiment. The purpose is to give the reader a better feeling for the procedure and the measured quantities. It should be possible to follow the calculations through.

The measurements described below serve two purposes: The first is to provide the necessary parameters to estimate the radiance using Eq. (5), and the second is to compare the values obtained with our radiometer with those obtained with a calibrated power meter. To estimate the radiance using Eq. (5) one must measure the (uncalibrated) spontaneous and stimulated output powers and the gain. The insertion loss to the EDF should also be measured accurately. To evaluate the gain, the output loss of the EDF must be measured, although the precision of this measurement is less critical. The raw data and the script containing all the calculations are included in the Supplemental Material [22].

A. Checking the absence of back-reflections

The return loss of fiber connections can be very high; however it is important to verify that this is below our desired measurement accuracy. In particular the EDF emits ASE in both directions; it is important that the back-emitted ASE is not back-reflected by the input components. To check this we disconnect the input of the EDF leaving the APC connector into a beam dump. We turn on the pump laser and measure the amount of light present at the output of the radiometer to be 10.84 μW. We then connect the input section (C2) and measure the amount of light again to be 10.81 μW. This small difference is due to a small reflection (3×10^{-4}) from the APC fiber face when it is not connected. This reflection is amplified by the gain when traveling backwards along the fiber. However, no back reflections seem to take place in the

equipment preceding C2. It is in order to conduct this test that we pump the EDF backwards rather than forwards.

B. Input and output losses

To measure output loss, light is fed through the EDF with the pump laser turned off. The amount of light at the output of the EDF (C3) is measured to be 14.12 nW. Connecting C3 we measure 9.889 nW at the output, so that the output transmission is $T_{\text{out}} = 0.7004$.

We evaluate the input loss at connector C1 by measuring the amount of light present in the input fiber before and after making the connection, obtaining 133.3 nW and 102.3 nW respectively, corresponding to a transmission of $T_{\text{C1}} = 0.7674$. This loss is mainly due to the WDM insertion loss. The input loss at C2 is measured by turning off the pump laser, injecting light from our source backward through the EDF and measuring the amount of light before and after making the C2 connection. We obtain 20.12 nW and 17.63 nW resulting in $T_{\text{C2}} = 0.8762$. The total input transmission will be $T_{\text{in}} = T_{\text{C1}} T_{\text{C2}} = 0.6725$. This relatively high loss is due to the different fiber mode field diameters employed in the setup.

C. Input power measurement

We measure the input power and spectrum at connector C1 with the power meter and spectrometer respectively. Although the power meter (Thorlabs PM100A with S154C head) is stable to four digits of precision, its reading is influenced by multiple reflections and interference between the fiber connector and detector faces. The reading is also affected by the type of connector used, FC-PC or FC-APC. We evaluated this error to be of the order of 2% to 4%.

The spectrum of the light which we inject into the radiometer is shown in Fig. 9 and the input power is measured at C1 to be 131.8 nW. When calculating the effective amount of light present at the input of the erbium-doped fiber, one must take into account the connection losses measured above. A disconnected fiber end has an output loss of nearly 4%, due to Fresnel reflection. One must therefore multiply values measured with the power meter by 1.038 in order to obtain the power in the fiber.
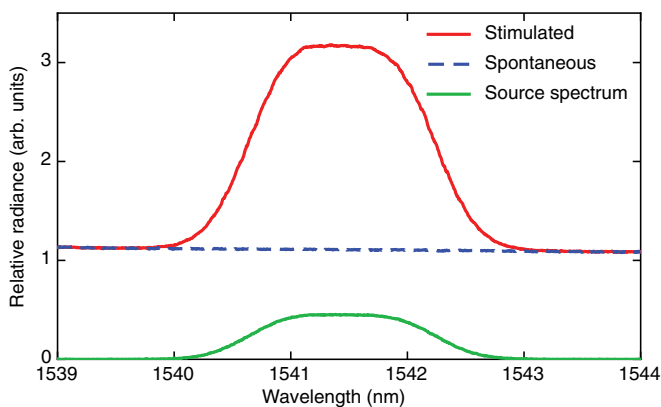

FIG. 9. (Color online) Relative spectra of the source light and spontaneous and stimulated emissions.

D. Measurement of the spontaneous and stimulated emissions

Figure 9 reports the spontaneous and stimulated emissions as measured by the spectrometer. To switch between the two we use the shutter which is integrated in the variable attenuator. We take care, using an isolator, that no back-reflections occur when the shutter is closed.

E. Measurement of the gain

The gain is measured by looking at the increase of output power with respect to the input power. In practice we measure the difference in spontaneous and stimulated emission of the radiometer with the power meter. We obtain 11.29 μW with the source off and 11.80 μW with the source on, giving a difference of 510 nW. Taking the output loss into consideration, this corresponds to 728 nW. Taking the input loss into account, P_{in} is 92 nW. Following Eq. (1) the gain has an average value of 7.9 over the spectrum of the input light. In our case the gain is close to flat over this spectrum. However, in general it is possible to deal with nonflat gain, as a spectral measurement of the spontaneous emission of the radiometer can yield the spectral gain. We can rewrite Eq. (1) as

$$G(\lambda) = \frac{\Delta P_{\text{out}}(\lambda)}{\Delta P_{\text{in}}(\lambda)} \tag{7a}$$

$$= \mu_{\text{out}}^{\text{sp}}(\lambda) + 1 \tag{7b}$$

$$= k' \, y_{\text{sp}}(\lambda) + 1, \tag{7c}$$

where $\mu_{\text{out}}^{\text{sp}}(\lambda)$ is the spectral radiance of the spontaneous emission of the radiometer and $y_{\text{sp}}(\lambda)$ is the reading of the spectrometer, while k' is a calibration constant. The mean gain $\bar{G}$ over the measured input power spectrum $k' \, P_{\text{in}}(\lambda)$ will be

$$\bar{G} = \frac{1}{\int_0^\infty P_{\text{in}}(\lambda)d\lambda} \int_0^\infty G(\lambda) P_{\text{in}}(\lambda)d\lambda \tag{8a}$$

$$= \frac{1}{\int_0^\infty P_{\text{in}}(\lambda)d\lambda} \int_0^\infty [k' \, y_{\text{sp}}(\lambda) + 1] P_{\text{in}}(\lambda)d\lambda. \tag{8b}$$

This equation can be solved for k':

$$k' = \int_0^\infty P_{\text{in}}(\lambda)d\lambda \frac{\bar{G} - 1}{\int_0^\infty P_{\text{in}}(\lambda) \, y_{\text{sp}}(\lambda)d\lambda}. \tag{9}$$

The mean gain $\bar{G}$ is measured with the power meter as described above, whereas $y_{\text{sp}}(\lambda)$ and $P_{\text{in}}(\lambda)$ are measured with the spectrometer. The obtained k value can then be used in Eq. (7c) to get the spectral gain $G(\lambda)$. Note that the contribution of the relative error on the gain to the error in μ_{in} goes with $1/G$.

F. Number of photons per mode of the source

Finally, all the parameters measured above can be put into Eq. (5) to obtain the spectral radiance in terms of number of photons per mode. The measured radiance is shown in Fig. 10, compared with the radiance measured by the combination of a calibrated power meter and the spectrometer, as described below.
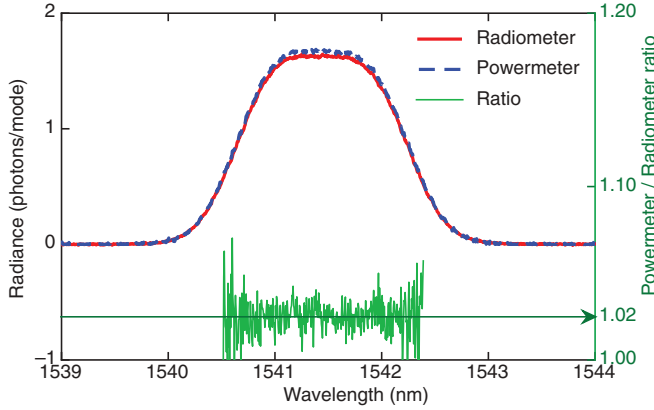
FIG. 10. (Color online) Comparison between the spectral radiance measured with the power meter and with the radiometer.

G. Comparison with a calibrated power meter

We compare the spectral radiance $\mu_{in}(\lambda)$ measured by the radiometer with that measured by a spectrometer normalized to a calibrated power meter, calculated as

$$\frac{P(\lambda)}{\Delta\lambda} = P_{in}^*(\lambda)\frac{P_{tot}}{\int_{-\infty}^{\infty} P_{in}^*(\lambda)\Delta\lambda}, \qquad (10)$$

where P_{tot} is measured with a power meter and serves to normalize the powers $P_{in}^*(\lambda)$ measured for each spectrometer "pixel" of width $\Delta\lambda$.

The number of temporal modes per second is the inverse of the coherence time $1/\tau_c = \Delta\nu$ as shown in Appendix A and in [16]. The fibers we use support a single spatial mode but two polarization modes so that the total number of modes per second is $N = 2\Delta\nu$. The number of photons per temporal mode in a small frequency bandwidth $\Delta\nu$ around frequency ν can then be calculated from the measured power spectral density $P(\lambda)/\Delta\nu$:

$$\mu(\lambda) = \frac{P(\lambda)}{2\,h\nu\,\Delta\nu} \qquad (11a)$$

$$= \frac{P(\lambda)\lambda^3}{2\,hc^2\,\Delta\lambda}. \qquad (11b)$$

It is interesting to note that the same result can be obtained with a different approach, detailed in Appendix B.

As described above, $P(\lambda)$ is calculated by multiplying the power measured with the power meter, by the normalized spectrum acquired with the spectrometer. The results are shown in Fig. 10. The radiometer measures a radiance which is 2% lower than that measured by the spectrometer plus power meter.

V. DISCUSSION

Although the absolute spectral radiance measured with the radiometer agrees with that measured with a power meter plus spectrometer combination (which has a 5% nominal error), to rule out systematic errors, this kind of measurement should be done with the techniques and equipment of a metrology laboratory. Here we can discuss the results in terms of linearity and stability, which we have measured with a slightly different technique: Instead of using the spectrometer discussed above
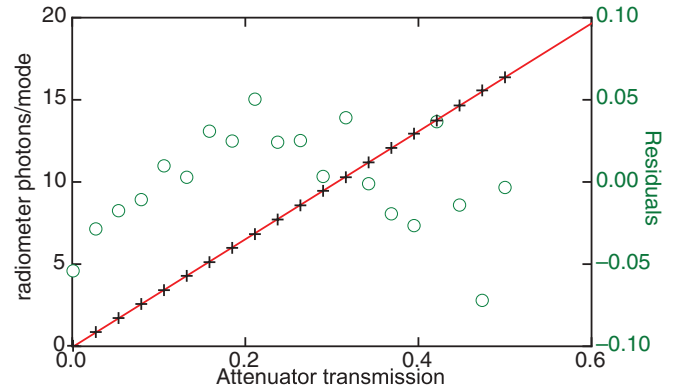

FIG. 11. (Color online) Linearity of our radiometer. Number of photons per mode measured by our radiometer versus transmission of the variable attenuator (linear scale). Residuals are magnified 100× and show no sign of saturation.

we selected a narrow spectral bandwidth with a filter, the rest of the treatment remaining identical.

A. Gain saturation and linearity

This method, unlike the radiometer described in [10], requires the entire erbium-doped fiber to be fully inverted under all operating conditions. Excess input light could deplete the number of atoms in the exited state and result in losses that are only present when P_{st} is being measured, and not when measuring P_{sp}. This nonlinearity will result in a systematic error to our measurement, and although it can be accounted for, it is best avoided. Figure 11 shows that our device is linear up to an input radiance of 15 photons per mode (the optimal operating point for the radiometer is 1 photon per mode, or ≈ 7 nW). The stability of the radiometer was measured over two hours and found to be of 10^{-4} as can be seen in Fig. 12.

B. Error estimation

Evaluating systematic errors is difficult because some sources of error may remain unnoticed. Loss mechanisms which we fail to take into account will influence our measurement in the same direction; i.e., we will always underestimate the input radiance.
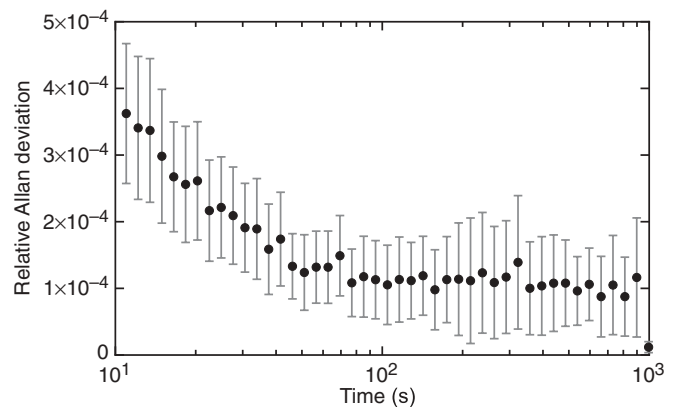

FIG. 12. Stability over a period of two hours: The Allan deviation drops to a value of 10^{-4}.

TABLE I. Summary of the uncertainties which play a direct role into our measurement of radiance. The starred (*) items only play a role when comparing our measured value of radiance with that of a power meter.

Parameter	Value	Uncertainty	Scaling	Effect
G	7.9	2%	$1/G$	0.25%
y_{st}/y_{sp}	2.9	$\approx 10^{-4}$%/dBm	y_{st}/y_{sp}	40 ppm
Insertion loss	0.67	0.16%	Linear	0.16%
Wavelength*	1541 nm	2 pm	λ^3	4 ppm
$\Delta\lambda$*	5 pm	100 ppm	Linear	100 ppm
PM calibration*	0.98	5%	Linear	5%

Table I includes an estimate of the error sources that we have evaluated, showing that this system has the potential of making an absolute measurement of radiance with an accuracy better than 1%. A better error analysis requires the resources of a metrology laboratory. We hope that this paper stimulates further work by a specialized team.

VI. CONCLUSION

In this work we demonstrated how a simple device capable of measuring the absolute spectral radiance can be built from standard telecom equipment. We have shown how limiting factors such as incomplete inversion and input loss estimation can be dealt with. This work provides sufficient detail to be reproduced independently and in particular to be developed and validated by a metrology laboratory.

ACKNOWLEDGMENTS

APPENDIX A: COHERENCE TIME OF A FREQUENCY ELEMENT $\Delta\nu$

Although we can trivially state that a frequency element $\Delta\nu$ has a coherence time of $1/\Delta\nu$, it is reassuring to derive this using a more general approach. Figure 13 shows the power spectral density of a small frequency element $\Delta\nu$ of our signal. We define this element as having a square shape which guarantees that there is no overlap between adjacent elements. The coherence time τ_0 is defined in terms of the autocorrelation function $\gamma(t)$ of the signal such that

$$\tau_0 = \int_{-\infty}^{\infty} |\gamma(t)|^2 dt. \tag{A1}$$

This definition of τ_c in not arbitrary but is a measurable physical quantity tied to the length $c\,\tau_c$ of the unit cell of photon phase space as described in [16].
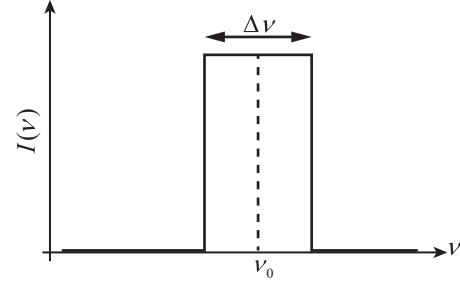

FIG. 13. Power spectral density function $I(\nu)$ for a small frequency element $\Delta\nu$ centered at ν_0.

The autocorrelation function $\gamma(t)$ is the Fourier transform of the power spectral density $I(\nu)$ so that

$$\gamma(t) = \int_{-\infty}^{\infty} I(\nu) e^{2\pi i t \nu} d\nu \tag{A2a}$$

$$= \frac{\sin(\pi t \Delta\nu)}{\pi t \Delta\nu}. \tag{A2b}$$

Integrating this function we obtain the coherence time:

$$\tau_0 = \int_{-\infty}^{\infty} \left| \frac{\sin(\pi t \Delta\nu)}{\pi t \Delta\nu} \right|^2 dt \tag{A3a}$$

$$= \frac{1}{\Delta\nu}, \tag{A3b}$$

which is the trivial result that we expected.

APPENDIX B: RADIANCE MEASURED WITH A POWER METER

In the text we estimate the radiance of our source using a power meter. The calculation relies on the definition of coherence time to count the number of modes per second. It is interesting to note that the same result can be obtained with a different approach. Consider Planck's blackbody radiation

$$B_\lambda(T) = \frac{2\,h\,c^2}{\lambda^5} \frac{1}{e^{hc/\lambda\,k\,T} - 1}. \tag{B1}$$

The last term can be identified as the number of photons per mode. Hence, the spectral radiance [in units of $W/(sr\,m^2)\,m^{-1}$] of a source with μ photons per mode can be written as

$$L_\lambda(\mu) = \frac{2\,h\,c^2}{\lambda^5} \mu. \tag{B2}$$

To obtain the spectral power density we multiply L_λ by the beam surface $\pi\,\omega^2$ and the solid angle $\pi\,\theta^2$ which for a Gaussian beam is λ^2. We can write this power spectral density as

$$\frac{P(\lambda)}{\Delta\lambda} = \frac{2\,h\,c^2}{\lambda^3} \mu(\lambda), \tag{B3}$$

which can be rewritten as

$$\mu(\lambda) = \frac{P(\lambda)\lambda^3}{2\,hc^2\,\Delta\lambda}, \tag{B4}$$

identical to Eq. (11b).

[1] J. E. Martin, N. P. Fox, and P. J. Key, Metrologia **21**, 147 (2005).

[2] D. H. Nettleton, *New Developments and Applications in Optical Radiometry*, Vol. 1 (IOP, Bristol, 1989), pp. 93–97.

[3] Jouni Envall, Petri Krh, and Erkki Ikonen, Metrologia **41**, 353 (2004).

[4] David J. Livigni, Nathan A. Tomlin, Christopher L. Cromer, and John H. Lehman, Metrologia **49**, S93 (2012).

[5] I. Vayshenker, D. J. Livigni, X. Li, J. H. Lehman, J. Li, L. M. Xiong, and Z. X. Zhang, J. Res. Natl. Inst. Stand. **115**, 433 (2010).

[6] J. Y. Cheung, C. J. Chunnilall, E. R. Woolliams, N. P. Fox, J. R. Mountford, J. Wang, and P. J. Thomas, J. Mod. Opt. **54**, 373 (2007).

[7] Joanne C. Zwinkels, Erkki Ikonen, Nigel P. Fox, Gerhard Ulm, and Maria Luisa Rastello, Metrologia **47**, R15 (2010).

[8] Sergey V. Polyakov and Alan L. Migdall, Opt. Express **15**, 1390 (2007).

[9] Jessica Y. Cheung, Christopher J. Chunnilall, Geiland Porrovecchio, Marek Smid, and Evangelos Theocharous, Opt. Express **19**, 20347 (2011).

[10] Bruno Sanguinetti, Enrico Pomarico, Pavel Sekatski, Hugo Zbinden, and Nicolas Gisin, Phys. Rev. Lett. **105**, 080503 (2010).

[11] D. N. Klyshko, Quantum Electron. **7**, 591 (1977).

[12] G. K. Kitaeva, A. N. Penin, V. V. Fadeev, and Y. A. Yanait, Sov. Phys. Dokl. **24**, 564 (1979).

[13] A. Migdall, E. Dauler, A. Muller, and A. Sergienko, Anal. Chim. Acta **380**, 311 (1999).

[14] Sergey V. Polyakov and Alan L. Migdall, J. Mod. Opt. **56**, 1045 (2009).

[15] Alan L. Migdall, Raju Datla, Alexander Sergienko, Jeffrey S. Orszak, and Yanhua H. Shih, Appl. Opt. **37**, 3455 (1998).

[16] L. Mandel and E. Wolf, Proc. Phys. Soc. **80**, 894 (1962).

[17] Edward F. Zalewski and C. Richard Duda, Appl. Opt. **22**, 2867 (1983).

[18] N. P. Fox, Metrologia **28**, 197 (1991).

[19] N. P. Fox, Metrologia **37**, 507 (2000).

[20] N. P. Fox, Metrologia **30**, 321 (2005).

[21] M. López, H. Hofer, and S. Kück, Metrologia **43**, 508 (2006).

[22] See Supplemental Material at http://link.aps.org/supplemental/10.1103/PhysRevA.86.062110 for raw data and script.